Equation of State for the Two-component Van der Waals Gas with Relativistic Excluded Volumes

G. Zeeb* †, K. A. Bugaev‡**, P. T. Reuter† and H. Stöcker†
† *Institut für Theoretische Physik, J.-W.-Goethe Universität Frankfurt am Main, Germany*
‡ *Gesellschaft für Schwerionenforschung mbH (GSI), Darmstadt, Germany*
** *Bogolyubov Institute for Theoretical Physics, 252143 Kiev, Ukraine*

A canonical partition function for the two-component excluded volume model is derived, leading to two different *van der Waals* approximations. The one is known as the *Lorentz-Berthelot* mixture and the other has been proposed recently. Both models are analysed in the canonical and grand canonical ensemble. In comparison with the one-component *van der Waals* excluded volume model the suppression of particle densities is reduced in these two-component formulations, but in two essentially different ways. Presently used multi-component models have no such reduction. They are shown to be not correct when used for components with different hard-core radii.
For high temperatures the excluded volume interaction is refined by accounting for the *Lorentz* contraction of the spherical excluded volumes, which leads to a distinct enhancement of lighter particles. The resulting effects on pion yield ratios are studied for AGS and SPS data.

KEYWORDS: Two-component and Multi-component Hadron Gas, Equation of State, Van der Waals Excluded Volume Model, Relativistic Excluded Volumes.

I. INTRODUCTION

Thermal models are commonly used to interprete experimental data from hadron collisions, see for instance [1–5]. In the *van der Waals* excluded volume *(VdW)* model the short range repulsion between particles is represented by hard-core potentials, i. e. the finite size of the particles is taken into account. As a consequence particle yields are essentially reduced in comparison with ideal gas results, whereas yield ratios remain almost unchanged, if the same hard-core radius is used for all particle species.

As particle species with smaller hard-core radii are closer to the ideal case, their particle densities are suppressed less. Consequently, their yield ratios to particle species with larger hard-core radii are enhanced. This fact has been used in recent efforts [6] to explain the experimentally observed pion abundance for AGS and SPS data [7] by introducing a smaller hard-core radius for pions R_π than for all other hadrons R_o. However, the resulting values are quite large, $R_\mathrm{o} = 0.8$ fm and $R_\pi = 0.62$ fm. In Ref. [8] a reasonable fit of SPS data has been obtained only for a distinctly smaller pair of hard-core radii.

The excluded volume models used in [6,8], however, are not correct in the case of different hard-core radii. As will be shown in Sect. II, these models correspond to a system where the components are separated from each other by a mobile wall and hence cannot mix.

A more realistic approach requires a two-component partition function including a term for the repulsion between particles of different hard-core radii. In the case of two components, however, the *VdW* approximation is not uniquely defined. The simplest possibility yields the *Lorentz-Berthelot* mixture, which was originally postulated by *van der Waals* for binary mixtures, see Refs. [9–12]. Another *VdW* approximation was recently proposed in Ref. [13]. These two formulations contain a suppression of particle densities similar to the one-component *van der Waals* gas, which is *reduced to different extend* for each formulation. In the present work we will study and apply both of these formulations.

There is yet another cause for a reduced excluded volume suppression. Particles are considered to be rigid spheres in the *VdW* model. At high energies as achieved in nuclear collisions, however, relativistic effects cannot be neglected [14]. Within the logic of the *VdW* model it is necessary to take into account the *Lorentz* contraction of the spheres. We will use an approach developed in Ref. [15] providing approximative formulae for relativistic excluded volumes: naturally, they decrease with rising temperature, and the effect is stronger for lighter particles. At high temperatures, consequently, it is not possible to use a *one-component VdW* description (i. e. a *common* excluded volume for *all* particle species) for a system of species with various masses. Since different masses cause different reductions of the excluded volumes at a given temperature, a *multi-component VdW* description is required.

To illustrate the influence of different excluded volumes we will restrict ourselves in this work to the simplest 'multi-component' case, the two-component case. The

*e-mail: gzeeb@th.physik.uni-frankfurt.de

crucial extension from the one- to the two-component case is to include the repulsion between particles of two *different* hard-core radii. As it will be illustrated, a generalisation to the multi-component case is straightforward and will yield no essential differences [16].

In the next section a derivation of the one-component canonical partition function with (constant) excluded volumes is presented. The generalisation to the two-component case is made and two possible *VdW* approximations are analysed: the *Lorentz-Berthelot* mixture [12] and the recently proposed approximation of Ref. [13]. The corresponding formulae for the grand canonical ensemble are derived and discussed in Sect. III. Relativistic excluded volumes are introduced in Sect. IV and the corresponding equations of state are presented for both models. In Sect. V a fit of particle yield ratios [6] is re-evaluated for both approximations, with constant and with relativistic excluded volumes. The conclusions are given in Sect. VI.

The appendixes A and C give a detailed analysis and comparison of the two approximations in the canonical and grand canonical ensemble, respectively. In App. B a general proof of the thermodynamical stability of the non-linear approximation is given.

II. CANONICAL TREATMENT

First we will derive the canonical partition function (CPF) for the one-component *VdW* gas by estimating the excluded volumes of particle clusters. Then this procedure will be generalised to the two-component case.

For simplicity *Boltzmann* statistics are used throughout this work. The deviations from quantum statistics are negligible as long as the density over temperature ratio is small. This is the case for the hadron gas at temperatures and densities typical for heavy ion collisions, see e. g. Ref. [6].

Note that in this work we will use the term *VdW* for the *van der Waals* excluded volume model, not for the general *van der Waals* model which includes attraction.

A. The Van der Waals Excluded Volume Model

Let us consider N identical particles with temperature T kept in a sufficiently large volume V, so that finite volume effects can be neglected. The partition function of this system ($\hbar = c = k_{\rm B} = 1$) reads

$$Z(T,V,N) = \frac{\phi^N}{N!} \int_{V^N} \mathrm{d}^3x_1 \ \cdots \ \mathrm{d}^3x_N \ \exp\left[-\tfrac{U_N}{T}\right] \ . \quad (1)$$

Here, $\phi \equiv \phi(T;m,g)$ denotes the momentum integral of the one particle partition

$$\phi(T;m,g) = \frac{g}{2\pi^2} \int\limits_0^\infty \mathrm{d}k \, k^2 \ \exp\left[-\tfrac{E(k)}{T}\right] \ , \quad (2)$$

where $E(k) \equiv \sqrt{k^2+m^2}$ is the relativistic energy and $g = (2S+1)(2I+1)$ counts the spin and isospin degeneracy. For a hard-core potential U_N of N spherical particles with radii R the potential term in Eq. (1) reads

$$\exp\left[-\tfrac{U_N}{T}\right] = \prod_{i<j\le N} \theta(|\vec{x}_{ij}| - 2R) \ , \quad (3)$$

where $\vec{x}_{ij}$ denotes the relative position vector connecting the centers of the i-th and j-th particle. Hence one can write

$$\begin{aligned}
&\int_{V^N} \mathrm{d}^3x_1 \ \cdots \ \mathrm{d}^3x_N \ \exp\left[-\tfrac{U_N}{T}\right] \\
&\quad = \int_{V^N} \mathrm{d}^3x_1 \ \cdots \ \mathrm{d}^3x_N \prod_{1\le i<j\le N} \theta(|\vec{x}_{ij}| - 2R) \\
&\quad = \int_V \mathrm{d}^3x_1 \int_V \mathrm{d}^3x_2 \ \theta(|\vec{x}_{12}| - 2R) \ \times \\
&\qquad \times \ \cdots \int_V \mathrm{d}^3x_N \prod_{1\le i\le N-1} \theta(|\vec{x}_{i,N}| - 2R) \\
&\quad \equiv \int_V \mathrm{d}^3x_1 \int^{\{\vec{x}_1\}} \mathrm{d}^3x_2 \ \cdots \int^{\{\vec{x}_1 \ldots \vec{x}_{N-1}\}} \mathrm{d}^3x_N \ . \quad (4)
\end{aligned}$$

Here, $\int^{\{\vec{x}_1 \ldots \vec{x}_j\}} \mathrm{d}^3x_{j+1}$ denotes the available volume for $\vec{x}_{j+1}$, which is the center of the particle with number $j+1$, if the j other particles are configurated as $\{\vec{x}_1 \ldots \vec{x}_j\}$. We will show now that this volume is estimated by $\int^{\{\vec{x}_1 \ldots \vec{x}_j\}} \mathrm{d}^3x_{j+1} \ge (V - 2b\,j)$, where $2b \equiv \frac{4\pi}{3}(2R)^3$ is the excluded volume of an isolated particle seen by a second one. Then, $2b\,j$ estimates the total volume which is excluded by all particle clusters occuring in the configuration $\{\vec{x}_1 \ldots \vec{x}_j\}$.

It is sufficient to prove that the excluded volume of a cluster of k particles is less than the excluded volume of k isolated particles. A group of k particles forms a k-cluster, if for any of these particles there is a neighbouring particle of this group at a distance less than $4R$. The *exact* excluded volume of a k-cluster, $v_{(k)}$, obviously depends on the configuration of the k particles. If one considers two isolated particles, i. e. two 1-clusters, and reduces their distance below $4R$, their excluded volumes will overlap. They form now a 2-cluster with the excluded volume $v_{(2)} = 4b - 1v_{\rm ov}$, where $v_{\rm ov}$ denotes the overlap volume.

Evidently, one can construct any k-cluster by attaching additional particles and calculate its excluded volume by subtracting each occuring overlap volume from $2b\,k$. It follows that $v_{(k)} < 2b\,k$ is valid for any k-cluster, and this inequality leads to the above estimate. Obviously, its accuracy improves with the diluteness of the gas.

Using these considerations one can approximate the r. h. s. of Eq. (4): starting with $j+1 = N$ one gradually replaces all integrals $\int^{\{\vec{x}_1 \ldots \vec{x}_j\}} \mathrm{d}^3x_{j+1}$ by $(V - 2b\,j)$. One has to proceed from the right to the left, because only the

respective rightmost of these integrals can be estimated in the described way. Hence one finds

$$Z(T,V,N) \geq \frac{\phi^N}{N!} \prod_{j=0}^{N-1} (V - 2b\,j) \ . \tag{5}$$

In this treatment the *VdW* approximation consists of two assumptions concerning Eq. (5) . Firstly, the product can be approximated by

$$\begin{aligned} \prod_{j=0}^{N-1} \left(1 - \tfrac{2b}{V}\, j\right) &\cong \exp\left[-\textstyle\sum_{j=0}^{N-1} \tfrac{2b}{V}\, j\right] \\ &= \exp\left[-\tfrac{b}{V}\,(N-1)N\right] \cong \left(1 - \tfrac{b}{V}\,N\right)^N \ , \end{aligned} \tag{6}$$

where $\exp[-x] \cong (1-x)$ is used for dilute systems, i. e. for low densities $2bN/V \ll 1$. The second assumption is to take the equality instead of the inequality in Eq. (5) . Then the CPF takes the *VdW* form,

$$Z_{\rm VdW}(T,V,N) = \frac{\phi^N}{N!}\ (V - bN)^N \ . \tag{7}$$

As usual, the *VdW* CPF is obtained as an approximation for dilute systems, but when used for high densities it should be considered as an *extrapolation*.

Finally, one obtains the well-known *VdW* pressure formula from the thermodynamical identity $p(T,V,N) \equiv T\,\partial \ln[Z(T,V,N)]/\partial V$,

$$p_{\,\rm VdW}(T,V,N) = \frac{T\,N}{V - bN} \ , \tag{8}$$

using the logarithm of the *Stirling* formula.

Now let us briefly investigate a system of volume V containing two components with *different* hard-core radii R_1 and R_2 which are separated by a wall and occupy the volume fractions xV and $(1-x)V$, respectively. According to Eq. (8) their pressures read

$$p_{\,\rm VdW}(T,xV,N_1) = \frac{T\,N_1}{xV - N_1 b_{11}} \ , \tag{9}$$

$$p_{\,\rm VdW}(T,(1-x)V,N_2) = \frac{T\,N_2}{(1-x)V - N_2 b_{22}} \ , \tag{10}$$

where the particle numbers N_1, N_2 and the excluded volumes $b_{11} = \frac{16\pi}{3}\,R_1^3$, $b_{22} = \frac{16\pi}{3}\,R_2^3$ correspond to the components 1 and 2 , respectively.

If the separating wall is mobile, the pressures (9) and (10) must be equal. In this case the fraction x can be eliminated and one obtains the common pressure of the whole system

$$\begin{aligned} p_{\,\rm VdW}(T,xV,N_1) &= p_{\,\rm VdW}(T,(1-x)V,N_2) \\ = \ p^{\,\rm sp}(T,V,N_1,N_2) &\equiv \frac{T\,(N_1+N_2)}{V - N_1 b_{11} - N_2 b_{22}} \ . \end{aligned} \tag{11}$$

Since the components are separated in this model system it will be referred to as the *separated* model [16] .

The pressure formula (11) corresponds to the *Boltzmann* approximation of the commonly used two-component *VdW* models of Refs. [6,8] as will be shown in Sect. V . It is evident that $p^{\,\rm sp}$ (11) does not describe the general two-component situation without a separating wall. Therefore, it is necessary to find a more realistic model, i. e. an approximation from a *two-component* partition function. This will be done in the following.

B. Generalisation to the Two-component Case

Recall the simple estimate (4–7) , which gives a physically transparent derivation of the one-component CPF in the *VdW* approximation. Let us use it now for a *two-component* gas of spherical particles with radii R_1 and R_2 , respectively. It is important to mention that each component may consist of several particle species as long as these species have one common hard-core radius, i. e. the number of necessary *VdW* components is determined by the number of different excluded volume terms b_{qq} . In the case of two radii the potential term (3) becomes

$$\begin{aligned} \exp\left[-\tfrac{U_{N_1+N_2}}{T}\right] \ = \ & \prod_{i<j\leq N_1} \theta(|\vec{x}_{ij}| - 2R_1) \times \\ & \times \prod_{k<\ell\leq N_2} \theta(|\vec{x}_{k\ell}| - 2R_2) \times \\ & \times \prod_{\substack{m\leq N_1 \\ n\leq N_2}} \theta(|\vec{x}_{mn}| - (R_1+R_2)) \ . \end{aligned} \tag{12}$$

The integration is carried out in the way described above; e. g. firstly over the coordinates of the particles of the second component, then over those of the first component. For the estimation of the excluded volume of a k-cluster now *two different* particle sizes have to be considered. One obtains

$$\begin{aligned} & Z(T,V,N_1,N_2) \\ & \geq \frac{\phi_1^{N_1}}{N_1!}\,\frac{\phi_2^{N_2}}{N_2!} \left\{\prod_{i=0}^{N_1-1} (V - 2b_{11}\,i)\right\} \times \\ & \quad \times \left\{\prod_{j=0}^{N_2-1} (V - 2b_{12}\,N_1 - 2b_{22}\,j)\right\} \\ & \cong \frac{\phi_1^{N_1}}{N_1!}\,\frac{\phi_2^{N_2}}{N_2!}\ V^{N_1+N_2} \times \\ & \quad \times \exp\left[-\tfrac{N_1^2 b_{11} + 2N_1 N_2 b_{12} + N_2^2 b_{22}}{V}\right] \ , \end{aligned} \tag{13}$$

where it is $\phi_q \equiv \phi(T; m_q, g_q)$, and $2b_{pq} \equiv \frac{4\pi}{3}\,(R_p + R_q)^3$ denotes the excluded volume of a particle of the component p seen by a particle of the component q ($p,\ q = 1,2$ hereafter) . Approximating the above exponent by $\exp[-x] \cong (1-x)$ yields the *simplest* possibility of a *VdW* approximation for the *two-component* CPF ,

$$Z^{\rm nl}_{\rm VdW}(T,V,N_1,N_2)$$

$$\equiv \frac{\phi_1^{N_1}}{N_1!}\,\frac{\phi_2^{N_2}}{N_2!}\,\times \tag{14}$$
$$\times\left(V-\frac{N_1^2 b_{11}+2N_1N_2b_{12}+N_2^2b_{22}}{N_1+N_2}\right)^{N_1+N_2}$$
$$=\frac{\phi_1^{N_1}}{N_1!}\,\frac{\phi_2^{N_2}}{N_2!}\,\times \tag{15}$$
$$\times\left(V-N_1b_{11}-N_2b_{22}+\frac{N_1\,N_2}{N_1+N_2}\,D\right)^{N_1+N_2}\quad,$$

where the non-negative coefficient D is given by

$$D\equiv b_{11}+b_{22}-2\,b_{12}\;. \tag{16}$$

This approximation will be called the *non-linear* approximation as the volume correction in (15) contains non-linear terms in N_1, N_2. The corresponding pressure follows from the thermodynamical identity,

$$p^{\,\mathrm{nl}}(T,V,N_1,N_2)\;=\;p_1^{\mathrm{nl}}+p_2^{\mathrm{nl}} \tag{17}$$
$$\equiv\frac{T\,(N_1+N_2)}{V-N_1b_{11}-N_2b_{22}+\frac{N_1\,N_2}{N_1+N_2}\,D}\quad.$$

This canonical formula corresponds to the *Lorentz-Berthelot* mixture (without attraction terms) known from the theory of fluids [12]. It was postulated by *van der Waals* [9] and studied as well by *Lorentz* [10] and *Berthelot* [11].

The crucial step from the one- to the two-component gas is to include b_{pq} terms ($p\neq q$) additionally to the $b_{qq}\equiv b|_{R=R_q}$ terms. For the multi-component gas no further essential extension is necessary. Consequently, the generalisation of the above procedure to the multi-component case, i. e. an arbitrary number of different hard-core radii, is straightforward [16].

In Ref. [13] a *more involved* approximation has been suggested for the two-component VdW gas. This follows from splitting the exponent in the CPF (13) by introducing *two generalised* excluded volume terms $\tilde b_{12}$ and $\tilde b_{21}$ (instead of a *single* and symmetric term $2\,b_{12}$) for the mixed case,

$$Z(T,V,N_1,N_2)$$
$$\cong\frac{\phi_1^{N_1}}{N_1!}\,\frac{\phi_2^{N_2}}{N_2!}\;V^{N_1+N_2}\,\times \tag{18}$$
$$\times\exp\left[-\frac{N_1^2b_{11}+N_1N_2\left(\tilde b_{12}+\tilde b_{21}\right)+N_2^2b_{22}}{V}\right]\quad,$$

which leads to an alternative two-component VdW CPF,

$$Z^{\mathrm{lin}}_{\mathrm{VdW}}(T,V,N_1,N_2)$$
$$\equiv\frac{\phi_1^{N_1}}{N_1!}\;\left(V-N_1b_{11}-N_2\tilde b_{21}\right)^{N_1}\,\times \tag{19}$$
$$\times\,\frac{\phi_2^{N_2}}{N_2!}\;\left(V-N_2b_{22}-N_1\tilde b_{12}\right)^{N_2}\quad.$$

Since the particle numbers N_1, N_2 appear solely linearly in the volume corrections, these formulae will be referred to as the *linear* approximation. In this approximation one obtains [13] for the pressure

$$p^{\,\mathrm{lin}}(T,V,N_1,N_2)\;=\;p_1^{\mathrm{lin}}+p_2^{\mathrm{lin}} \tag{20}$$
$$\equiv\frac{T\,N_1}{V-N_1b_{11}-N_2\tilde b_{21}}+\frac{T\,N_2}{V-N_2b_{22}-N_1\tilde b_{12}}\quad.$$

The choice of the generalised excluded volume terms $\tilde b_{pq}$ is not unique in the sense that all choices which satisfy the basic constraint $\tilde b_{12}+\tilde b_{21}=2b_{12}$ are consistent with the second order virial expansion [13]. Therefore, additional conditions are necessary to fix these generalised excluded volumes. In Ref. [13] they were chosen as

$$\tilde b_{12}\equiv b_{11}\,\frac{2\,b_{12}}{b_{11}+b_{22}}\;,\quad \tilde b_{21}\equiv b_{22}\,\frac{2\,b_{12}}{b_{11}+b_{22}}\;. \tag{21}$$

For this choice, the linear approximation reproduces a traditional VdW gas behaviour, i. e. *one-component-like*, in the two limits $R_2=R_1$ and $R_2=0$ as readily checked. The factor $2b_{12}/(b_{11}+b_{22})=1-D/(b_{11}+b_{22})$ is always smaller than unity for $R_1\neq R_2$, consequently, the $\tilde b_{pq}$ terms are smaller than the corresponding terms b_{pp}. Note that there are many possible choices for $\tilde b_{12}$ and $\tilde b_{21}$, e. g. additionally dependent on the particle numbers N_1 and N_2, whereas the non-linear approximation (14) contains no such additional parameters.

The formulae of the linear approximation are generally valid for *any* choice of $\tilde b_{12}$ and $\tilde b_{21}$ satisfying the constraint $\tilde b_{12}+\tilde b_{21}=2b_{12}$. In the following, however, we will restrict our study to the special choice given in the Eqs. (21). The canonical (and grand canonical) formulae for the multi-component case are given in Ref. [13].

C. Comparison of both Two-component VdW Approximations

As the VdW approximation is a low density approximation it is evident that the linear and non-linear formulae are equivalent for such densities. Deviations, however, occur at high densities, where any VdW approximation generally becomes inadequate.

The differences between both approximations result from the fact that the linear pressure (20) has two poles, $v_1^{\mathrm{lin}}=V$ and $v_2^{\mathrm{lin}}=V$, whereas the non-linear pressure (17) has solely one pole, $v^{\,\mathrm{nl}}=V$. For constant volume V these poles define limiting densities, e. g. $\hat n_1=\max(N_1/V)$ as functions of $n_2=N_2/V$,

$$v_q^{\,\mathrm{lin}}(N_1,N_2)=V\quad\rightsquigarrow\quad\hat n_1(n_2)\equiv\hat n_{1,q}^{\,\mathrm{lin}}(n_2) \tag{22}$$
$$\text{or}\quad v^{\,\mathrm{nl}}(N_1,N_2)=V\quad\rightsquigarrow\quad\hat n_1(n_2)\equiv\hat n_1^{\,\mathrm{nl}}(n_2)\;, \tag{23}$$

which represent the domains of the two pressure formulae in the n_2–n_1-plane. The explicit fomulae are discussed in App. A.

In Fig. 1 (a) an example of these limiting densities is shown for $R_2/R_1=0.4$. It is clearly seen that the non-linear domain (below the solid line) is larger than the

linear domain (below both dashed lines), which is generally the case for $R_2 \neq R_1$. Especially for $R_2 \ll R_1$ the non-linear domain is distinctly larger for high densities of the large component, $n_1 b_{11} > n_2 b_{22}$, whereas both domains are similar for high densities of the small component, $n_2 b_{22} > n_1 b_{11}$.

The linear approximation is constructed in traditional *VdW* spirit; the densities n_q^{lin} achieved in this approximation are below the maximum density of the corresponding *one-component VdW* gas $\max(n_q^{\mathrm{oc}}) = 1/b_{qq}$, which is defined by the pole of $p_q^{\mathrm{oc}} \equiv p_{\mathrm{VdW}}(T, V, N_q; b_{qq})$ from Eq. (8).

In the non-linear approximation, however, the possible densities of the larger particles n_1^{nl} can exceed $1/b_{11}$ due to the occurence of negative partial derivatives of the pressure, $\partial p^{\mathrm{nl}}/\partial N_2 < 0$. In this context it is necessary to state that this behaviour does not lead to a thermodynamical instability of the non-linear approximation as proven in App. B. The linear approximation shows no such behaviour, it is always $\partial p^{\mathrm{lin}}/\partial N_1 > 0$ and $\partial p^{\mathrm{lin}}/\partial N_2 > 0$.

The condition $\partial p^{\mathrm{nl}}/\partial N_2 = 0$ defines the boundary $\hat{n}_1^{\mathrm{nl,\,bd}}(n_2)$ of the region of negative partial derivatives of the non-linear pressure. In Fig. 1 (a) this boundary is shown by the dotted line for $R_2/R_1 = 0.4$; the values of $\partial p^{\mathrm{nl}}/\partial N_2$ are negative above this line.

Densities larger than $n_1^{\mathrm{nl}} = 1/b_{11}$ can only occur, if R_2 is smaller than a critical radius,

$$R_2 < R_{2,\,\mathrm{crit}}(R_1) = (\sqrt[3]{4} - 1)\, R_1 \approx R_1/1.7\,. \qquad (24)$$

Then, the boundary $\hat{n}_1^{\mathrm{nl,\,bd}}(n_2)$ starts inside the non-linear domain, see App. A for details.

The reason for this behaviour is the ratio of the amounts of small and large particles. There are much more small than large particles in the system for densities n_1, n_2 along the boundary $\hat{n}_1^{\mathrm{nl,\,bd}}(n_2)$ at high densities n_1: here, the fewer large particles are surrounded by many small particles. Therefore, the excluded volume interaction of the large particles in the non-linear pressure (17) is governed not by the simple term b_{11} but by the mixed term b_{12}, which is distinctly smaller than b_{11} for $R_2 \ll R_1$. The maximum density achieved in the non-linear approximation $\max(\hat{n}_1^{\mathrm{nl}}) = 4/b_{11}$ is obtained for $R_2 \to 0$ and $N_2 \gg N_1$, i. e. these formulae go far *beyond* the traditional *VdW* results in the corresponding situation.

An example of pressure profiles for p_1^{lin}, p_2^{lin} and p^{nl} for $n_1 b_{11} = 0.9$ is shown in Fig. 1 (b), where it is $R_2/R_1 = 0.4$ as in Fig. 1 (a). The non-linear pressure (solid line) firstly decreases as the densities n_1, n_2 correspond to the region of negative partial derivatives, see Fig. 1 (a). The partial pressures of the linear approximation are shown by dashed lines. The non-linear domain is seen to be larger since it is one of the linear partial pressures which diverges first for increasing n_2.

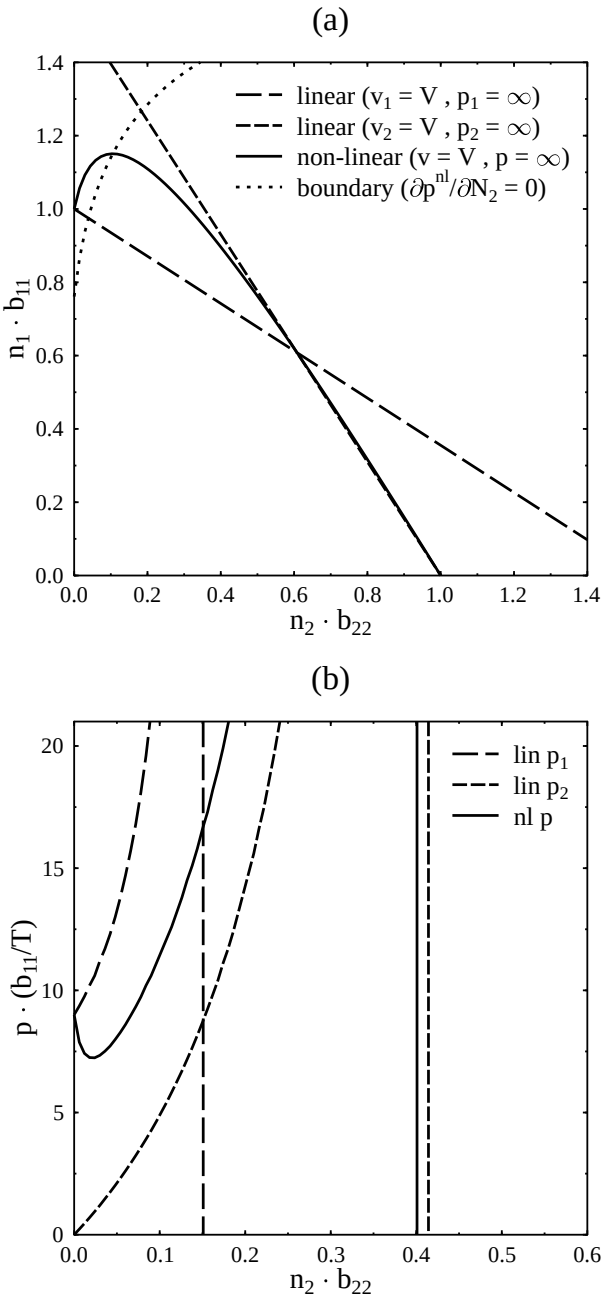

FIG. 1. (a) Domains of the linear and non-linear approximation for $R_2/R_1 = 0.4$: limiting densities $\hat{n}_1$ (isobars for $p_q(n_1, n_2) = \infty$) and the lower boundary $\hat{n}_1^{\mathrm{nl,\,bd}}$ to the region of negative partial derivatives of the non-linear pressure. The dashed lines correspond to the two poles of the linear pressure, and the solid line corresponds to the pole of the non-linear pressure. For given n_2 the possible densities n_1^{lin} are below both dashed lines, whereas the possible densities n_1^{nl} are below the solid line. Negative derivatives $\partial p^{\mathrm{nl}}/\partial N_2 < 0$ occur only above the dotted line.
(b) Pressure profiles in dimensionless units for $R_2/R_1 = 0.4$ as in (a) at fixed $n_1 b_{11} = 0.9$. The dashed lines show the partial pressures of the linear approximation p_1^{lin} and p_2^{lin}, while the solid line shows the total pressure of the non-linear approximation p^{nl} with initial decrease due to negative $\partial p^{\mathrm{nl}}/\partial N_2$.

We conclude that the linear and non-linear approximation show a drastically different behaviour for high values of the large component's density n_1. In the linear approximation (20) the possible density values are below $1/b_{11}$ and $1/b_{22}$, respectively, and the derivatives $\partial p^{\rm lin}/\partial N_q$ are always positive. Whereas in the non-linear approximation (17) higher densities $n_1 > 1/b_{11}$ are possible due to the occurence of negative derivatives $\partial p^{\rm nl}/\partial N_2 < 0$. This may be considered as pathological – or used as an advantage to describe special situations, e. g. densities $1/b_{11} < n_1 < \hat{n}_1^{\rm nl}$ for $R_2 \ll R_1$ (see App. A).

However, the use of any VdW approximation is in principle problematic for densities near $1/b_{qq}$. For low densities the non-linear and linear approximation are practically equivalent, and the non-linear approximation is preferable since the formulae are essentially simpler.

III. GRAND CANONICAL TREATMENT

Let us now turn to the grand canonical ensemble (GCE). The grand canonical partition function is built using the CPF,

$$\mathcal{Z}(T,V,\mu_1,\mu_2) = \sum_{N_1=0}^{\infty}\sum_{N_2=0}^{\infty} \exp\left[\tfrac{\mu_1 N_1+\mu_2 N_2}{T}\right] Z(T,V,N_1,N_2)\ , \tag{25}$$

whereas the chemical potentials μ_1 and μ_2 correspond to the components 1 and 2, respectively. For the VdW CPF (15) or (19) there are limiting particle numbers $\hat{N}_1(N_2)$ or $\hat{N}_2(N_1)$, where each CPF becomes zero. For this reason the above sum contains only a finite number of terms. Then it can be shown that in the thermodynamical limit (i. e. in the limit $V \to \infty$ for $N_q/V = \text{const.}$) the grand canonical pressure $p(T,\mu_1,\mu_2) \equiv T\ \ln[\mathcal{Z}(T,V,\mu_1,\mu_2)]/V$ depends only on the *maximum term* of the double sum (25), where $N_1 = \mathcal{N}_1$ and $N_2 = \mathcal{N}_2$. One obtains

$$p(T,\mu_1,\mu_2) = \lim_{V\to\infty}\frac{T}{V}\ \ln\left[\exp\left[\tfrac{\mu_1\mathcal{N}_1+\mu_2\mathcal{N}_2}{T}\right] Z(T,V,\mathcal{N}_1,\mathcal{N}_2)\right]\ , \tag{26}$$

wheras $\mathcal{N}_1$ and $\mathcal{N}_2$ are the *average* particle numbers.

A. The Two VdW Approximations

For the non-linear VdW approximation (15) the last expression takes the form

$$p^{\rm nl}(T,\mu_1,\mu_2) = \lim_{V\to\infty}\frac{T}{V}\ \ln\left[\tfrac{A_1^{\mathcal{N}_1}}{\mathcal{N}_1!}\ \tfrac{A_2^{\mathcal{N}_2}}{\mathcal{N}_2!}\ \times \right. \left. \times\left(V-\mathcal{N}_1 b_{11}-\mathcal{N}_2 b_{22}+\tfrac{\mathcal{N}_1\mathcal{N}_2}{\mathcal{N}_1+\mathcal{N}_2}\,D\right)^{\mathcal{N}_1+\mathcal{N}_2}\right]\ , \tag{27}$$

where $A_q = A(T,\mu_q;\ m_q,g_q) \equiv \exp[\mu_q/T]\ \phi_q$.

The evaluation of both maximum conditions for the grand canonical pressure

$$0 \stackrel{!}{=} \frac{\partial}{\partial\mathcal{N}_q}\left\{\ln\left[\tfrac{A_1^{\mathcal{N}_1}}{\mathcal{N}_1!}\ \tfrac{A_2^{\mathcal{N}_2}}{\mathcal{N}_2!}\ \times \right. \left. \times\left(V-\mathcal{N}_1 b_{11}-\mathcal{N}_2 b_{22}+\tfrac{\mathcal{N}_1\mathcal{N}_2}{\mathcal{N}_1+\mathcal{N}_2}\,D\right)^{\mathcal{N}_1+\mathcal{N}_2}\right]\right\}\ , \tag{28}$$

yields a system of two coupled transcendental equations,

$$\xi_1^{\rm nl}(T,\mu_1,\mu_2) = A_1\ \exp\left[-(\xi_1^{\rm nl}+\xi_2^{\rm nl})\,b_{11}+\tfrac{\xi_2^{\rm nl\,2}}{\xi_1^{\rm nl}+\xi_2^{\rm nl}}\,D\right]\ , \tag{29}$$

$$\xi_2^{\rm nl}(T,\mu_1,\mu_2) = A_2\ \exp\left[-(\xi_1^{\rm nl}+\xi_2^{\rm nl})\,b_{22}+\tfrac{\xi_1^{\rm nl\,2}}{\xi_1^{\rm nl}+\xi_2^{\rm nl}}\,D\right]\ , \tag{30}$$

where $\xi_1^{\rm nl}$ and $\xi_2^{\rm nl}$ are defined as

$$\xi_1^{\rm nl} \equiv \frac{\mathcal{N}_1}{V-\mathcal{N}_1 b_{11}-\mathcal{N}_2 b_{22}+\frac{\mathcal{N}_1\mathcal{N}_2}{\mathcal{N}_1+\mathcal{N}_2}\,D}\ , \tag{31}$$

$$\xi_2^{\rm nl} \equiv \frac{\mathcal{N}_2}{V-\mathcal{N}_1 b_{11}-\mathcal{N}_2 b_{22}+\frac{\mathcal{N}_1\mathcal{N}_2}{\mathcal{N}_1+\mathcal{N}_2}\,D}\ . \tag{32}$$

In the thermodynamical limit the average particle numbers $\mathcal{N}_1$ and $\mathcal{N}_2$ are proportional to V as $\mathcal{N}_q = n_q^{\rm nl}\,V$. Then the volume V disappears in the definitions of $\xi_1^{\rm nl}$ and $\xi_2^{\rm nl}$ given by Eqs. (31, 32), and they can be solved for either the density $n_1^{\rm nl}$ or $n_2^{\rm nl}$,

$$n_1^{\rm nl}(T,\mu_1,\mu_2) = \frac{\xi_1^{\rm nl}}{1+\xi_1^{\rm nl}b_{11}+\xi_2^{\rm nl}b_{22}-\frac{\xi_1^{\rm nl}\xi_2^{\rm nl}}{\xi_1^{\rm nl}+\xi_2^{\rm nl}}\,D}\ , \tag{33}$$

$$n_2^{\rm nl}(T,\mu_1,\mu_2) = \frac{\xi_2^{\rm nl}}{1+\xi_1^{\rm nl}b_{11}+\xi_2^{\rm nl}b_{22}-\frac{\xi_1^{\rm nl}\xi_2^{\rm nl}}{\xi_1^{\rm nl}+\xi_2^{\rm nl}}\,D}\ . \tag{34}$$

The $\xi_q^{\rm nl} = \xi_q^{\rm nl}(T,\mu_1,\mu_2)$ are the solutions of the coupled Eqs. (29) and (30), respectively.

Hence, the pressure (27) can be rewritten in terms of $\xi_1^{\rm nl}$ (29) and $\xi_2^{\rm nl}$ (30),

$$p^{\rm nl}(T,\mu_1,\mu_2) = T\ \left(\xi_1^{\rm nl}+\xi_2^{\rm nl}\right)\ , \tag{35}$$

supposed that Eqs. (33, 34) are taken into account. If the definitions (31) and (32) are used for $\xi_1^{\rm nl}$ and $\xi_2^{\rm nl}$, the pressure formula (35) coincides with the canonical expression (17) for $N_1 = \mathcal{N}_1$ and $N_2 = \mathcal{N}_2$.

Since the formulation is thermodynamically self-consistent the identity $n_q \equiv \partial p(T,\mu_1,\mu_2)/\partial\mu_q$ leads to Eqs. (33, 34) as well.

The grand canonical formulae of the linear approximation [13] are obtained exactly as presented for the non-linear case in Eqs. (27–35). In the linear case the two coupled transcendental equations are

$$\xi_1^{\rm lin}(T,\mu_1,\mu_2) = A_1 \ \exp\left[-\xi_1^{\rm lin}\, b_{11} - \xi_2^{\rm lin}\, \tilde{b}_{12}\right] \ , \qquad (36)$$

$$\xi_2^{\rm lin}(T,\mu_1,\mu_2) = A_2 \ \exp\left[-\xi_2^{\rm lin}\, b_{22} - \xi_1^{\rm lin}\, \tilde{b}_{21}\right] \ , \qquad (37)$$

with the definitions

$$\xi_1^{\rm lin} \equiv \frac{\mathcal{N}_1}{V - \mathcal{N}_1 b_{11} - \mathcal{N}_2 \tilde{b}_{21}} \ , \qquad (38)$$

$$\xi_2^{\rm lin} \equiv \frac{\mathcal{N}_2}{V - \mathcal{N}_2 b_{22} - \mathcal{N}_1 \tilde{b}_{12}} \ . \qquad (39)$$

The expressions for the particle densities are found by solving Eqs. (38, 39) for either $n_1^{\rm lin}$ or $n_2^{\rm lin}$,

$$n_1^{\rm lin}(T,\mu_1,\mu_2) \qquad (40)$$
$$= \frac{\xi_1^{\rm lin}(1+\xi_2^{\rm lin}\,[b_{22}-\tilde{b}_{21}])}{1+\xi_1^{\rm lin} b_{11}+\xi_2^{\rm lin} b_{22}+\xi_1^{\rm lin}\xi_2^{\rm lin}\,[b_{11}b_{22}-\tilde{b}_{12}\tilde{b}_{21}]} \ ,$$

$$n_2^{\rm lin}(T,\mu_1,\mu_2) \qquad (41)$$
$$= \frac{\xi_2^{\rm lin}(1+\xi_1^{\rm lin}\,[b_{11}-\tilde{b}_{12}])}{1+\xi_1^{\rm lin} b_{11}+\xi_2^{\rm lin} b_{22}+\xi_1^{\rm lin}\xi_2^{\rm lin}\,[b_{11}b_{22}-\tilde{b}_{12}\tilde{b}_{21}]} \ .$$

For the linear approximation the pressure (26) can be rewritten in terms of $\xi_1^{\rm lin}$ (36) and $\xi_2^{\rm lin}$ (37),

$$p^{\,\rm lin}(T,\mu_1,\mu_2) = T\ \left(\xi_1^{\rm lin}+\xi_2^{\rm lin}\right) \ , \qquad (42)$$

if Eqs. (40, 41) are taken into account, like in the non-linear case.

B. Comparison of both Approximations

Let us briefly return to the usual *VdW* case, the one-component case. The corresponding transcendental equation is obtained from either Eqs. (29, 30) or (36, 37) by setting $R_1 = R_2 \equiv R$ and $A_1 = A_2 \equiv A$,

$$\xi^{\,\rm oc}(T,\mu) = A\,\exp\left[-\xi^{\,\rm oc}\, b\right] \ , \qquad (43)$$

whereas $b \equiv b_{11} = b_{22}$. The *transcendental factor* $\exp[-\xi^{\,\rm oc}\, b]$ has the form of a suppression term, and the solution $\xi^{\,\rm oc} \equiv p^{\,\rm oc}/T$ of this transcendental equation evidently decreases with increasing b for constant T and μ. Then in turn, the corresponding particle density $n^{\,\rm oc} = \xi^{\,\rm oc}/(1+\xi^{\,\rm oc}\, b)$ is suppressed in comparison with the ideal gas due to the lower $\xi^{\,\rm oc}$ *and* the additional denominator. Thus, a suppressive transcendental factor corresponds to a suppression of particle densities.

Now it can be seen from Eqs. (29, 30) and (36, 37) that the transcendental factors of both *two-component* approximations contain as well this usual *one-component*- or *VdW-like* suppressive part $\exp[-(p/T)\, b_{qq}]$. But since it is $D \geq 0$ and $\tilde{b}_{pq} < b_{pp}$, respectively, there is furthermore an attractive part in each corresponding transcendental factor.

In the non-linear approximation the attractive part can even dominate the suppressive part for the smaller component, e. g. in Eq. (30) for $R_2 < R_1$. Then the larger component can reach densities $n_1^{\rm nl}$ higher than $1/b_{11}$, analogous to the CE. A detailed discussion is given in App. C.

High densities in the canonical treatment correspond to large values of the chemical potentials in the grand canonical treatment. In the limit

$$\mu_1/T \to \infty \ \ (T, \mu_2 = \text{const.}) \quad \text{or} \quad \xi_1^{\rm nl} \to \infty \qquad (44)$$

the solution of Eq. (30), $\xi_2^{\rm nl}$, can be enhanced for increasing $\xi_1^{\rm nl}$ instead of being suppressed, if R_2 is sufficiently small. This may be called the *non-linear enhancement*. The behaviour of the non-linear approximation in the limit (44) depends only on the ratio of the two radii R_1/R_2 and is characterised by the coefficient

$$a_2 \equiv \sqrt{D/b_{22}} - 1 \ . \qquad (45)$$

A negative a_2 relates to a suppressive transcendental factor in Eq. (30). For equal radii $R_2 = R_1$ it is $a_2 = -1$, and the suppression is evidently not reduced but *VdW*-like. For $-1 < a_2 < 0$ this suppression is reduced, the most strongly for $a_2 \approx 0$.

In the case $a_2 = 0$ the suppression for $\xi_2^{\rm nl}$ (30) disappears in the limit (44), on has $\xi_2^{\rm nl} \to A_2 = \text{const}$. This case provides the critical radius $R_{2,\,\rm crit}$ (24).

For $a_2 > 0$ or $R_2 < R_{2,\,\rm crit}$ the non-linear enhancement of $\xi_2^{\rm nl}$ occurs for increasing $\xi_1^{\rm nl}$; it is the stronger the larger a_2 is. Then $n_1^{\rm nl}$ (33) can exceed $\max(n_1^{\rm oc}) = 1/b_{11}$, whereas $n_2^{\rm nl}$ (34) does not vanish (see App. C for the explicit fomulae). The density $\max(\hat{n}_1^{\rm nl}) = 4/b_{11}$ is achieved for $a_2 \to \infty$ or $R_2 \to 0$.

The suppression in the transcendental factor of $\xi_1^{\rm nl}$ (29) is generally reduced for $R_2 < R_1$, the more strongly the smaller R_2 is, but there is no enhancement possible in the limit (44).

IV. RELATIVISTIC EXCLUDED VOLUMES

In this section we will investigate the influence of relativistic effects on the excluded volumes of fast moving particles by accounting for their ellipsoidal shape due to *Lorentz* contraction. In Ref. [15] a quite simple, ultra-relativistic approach has been made to estimate these effects: instead of ellipsoids two cylinders with the corresponding radii have been used to calculate approximately the excluded volume term b_{pq} for the two-component mixture. The resulting relativistic excluded volumes depend on the temperature and contain the radii and the *masses* as parameters. The simple, non-mixed term reads [14]

$$b_{qq}(T) = \alpha_{qq}\left(\frac{37\pi}{9}\,\frac{\sigma_q}{\phi_q} + \frac{\pi^2}{2}\right) R_q^3 \ , \qquad (46)$$

where $\sigma_q \equiv \sigma(T; m_q, g_q)$ denotes the *ideal gas* scalar density,

$$\sigma(T;m,g) = \frac{g}{2\pi^2} \int\limits_0^\infty \mathrm{d}k\, k^2\, \frac{m}{E(k)}\, \exp\left[-\tfrac{E(k)}{T}\right] \ . \qquad (47)$$

The expression for the mixed case can be derived similarly from [15],

$$b_{12}(T) = \alpha_{12} \left\{ \left(\tfrac{\sigma_1}{\phi_1}\, f_1 + \tfrac{\pi^2}{4}\, \tfrac{R_2}{R_1} \right) R_1^3 + \left(\tfrac{\sigma_2}{\phi_2}\, f_2 + \tfrac{\pi^2}{4}\, \tfrac{R_1}{R_2} \right) R_2^3 \right\} \ , \qquad (48)$$

whereas the abbreviations f_1 and f_2 are dimensionless functions of both radii,

$$f_1 = \tfrac{\pi}{3} \left(2 + \tfrac{3R_2}{R_1} + \tfrac{7R_2^2}{6R_1^2} \right) \ , \quad f_2 = \tfrac{\pi}{3} \left(2 + \tfrac{3R_1}{R_2} + \tfrac{7R_1^2}{6R_2^2} \right) \ .$$

The normalisation factors

$$\alpha_{11} = \alpha_{22} = \frac{16}{\frac{37}{3} + \frac{3\pi}{2}} \ , \qquad (49)$$

$$\alpha_{12} = \frac{\frac{2\pi}{3}(R_1+R_2)^3}{\left(f_1 + \frac{\pi^2}{4}\frac{R_2}{R_1} \right) R_1^3 + \left(f_2 + \frac{\pi^2}{4}\frac{R_1}{R_2} \right) R_2^3} \qquad (50)$$

are introduced to normalise the ultra-relativistic approximations (46, 48) for $T = 0$ to the corresponding non-relativistic results. For the hadron gas, however, these *Boltzmann* statistical formulae will only be used at high temperatures, where effects of quantum statistics are negligible.

Note that it is *not appropriate* to consider temperature dependent hard-core radii $R_p(T)$ or $R_q(T)$ since the $b_{pq}(T)$ terms give the *Lorentz*-contracted excluded *volumes* and are involved functions of T, m_p, m_q, R_p and R_q. However, for a given value of $b_{pq}(T)$ the necessary hard-core radii R_p and R_q will obviously depend on the temperature.

It is evident that the formulae (46, 48) suffice already for the multi-component case, because even a multi-component *VdW* formulation contains only b_{pq} terms.

For both approximations the expressions for the pressure (35) or (42) and corresponding particle densities (33, 34) or (40, 41) remain unchanged. However, due to the temperature dependence of the relativistic excluded volumes the entropy density is modified

$$s(T,\mu_1,\mu_2) \equiv \frac{\partial}{\partial T}\, p(T,\mu_1,\mu_2) \equiv s_{\mathrm{nrel}} + s_{\mathrm{rel}}(\partial_T b_{11}, \partial_T b_{22}, \partial_T b_{12}) \ . \qquad (51)$$

The additional term s_{rel} depends on temperature derivatives of the relativistic excluded volumes, $\partial_T b_{pq} \equiv \partial b_{pq}/\partial T$, which represent their thermal compressibility.

Furthermore, the term s_{rel} generates additional terms for the energy density, according to $e \equiv Ts - p + \mu_1 n_1 + \mu_2 n_2$. In the non-linear approximation one obtains

$$e^{\,\mathrm{nl}}(T,\mu_1,\mu_2) = n_1^{\mathrm{nl}}\, \frac{\epsilon_1}{\phi_1} + n_2^{\mathrm{nl}}\, \frac{\epsilon_2}{\phi_2} - (n_1^{\mathrm{nl}} + n_2^{\mathrm{nl}})\, T^2 \times \left(\xi_1^{\mathrm{nl}}\, \partial_T b_{11} + \xi_2^{\mathrm{nl}}\, \partial_T b_{22} - \tfrac{\xi_1^{\mathrm{nl}}\, \xi_2^{\mathrm{nl}}}{\xi_1^{\mathrm{nl}} + \xi_2^{\mathrm{nl}}}\, \partial_T D \right) \ , \qquad (52)$$

and the linear approximation yields

$$e^{\,\mathrm{lin}}(T,\mu_1,\mu_2) = n_1^{\mathrm{lin}}\, \frac{\epsilon_1}{\phi_1} + n_2^{\mathrm{lin}}\, \frac{\epsilon_2}{\phi_2} - n_1^{\mathrm{lin}}\, T^2 \left(\xi_1^{\mathrm{lin}}\, \partial_T b_{11} + \xi_2^{\mathrm{lin}}\, \partial_T \tilde{b}_{12} \right) - n_2^{\mathrm{lin}}\, T^2 \left(\xi_2^{\mathrm{lin}}\, \partial_T b_{22} + \xi_1^{\mathrm{lin}}\, \partial_T \tilde{b}_{21} \right) \ , \qquad (53)$$

whereas $\epsilon_q \equiv \epsilon(T; m_q, g_q)$ denotes the *ideal gas* energy density

$$\epsilon(T;m,g) = \frac{g}{2\pi^2} \int\limits_0^\infty \mathrm{d}k\, k^2\, E(k)\, \exp\left[-\tfrac{E(k)}{T}\right] \ . \qquad (54)$$

The additional terms in the entropy density (51) and in the energy density (52) or (53) which contain temperature derivatives do evidently not occur in the case of the usual non-relativistic, i. e. constant excluded volumes.

Let us now study the hadronic equation of state generated by each of the two-component *VdW* approximations and their modifications due to relativistic excluded volumes. When used to describe *hadronic* particles, the hard-core radii R_q should be considered as *parameters* rather than particle radii. We identify the first component as nucleons ($m_1 \equiv m_{\mathrm{n}} = 939$ MeV, $\mu_1 \equiv \mu_{\mathrm{n}} = \mu_{\mathrm{B}}$ and $g_1 \equiv g_{\mathrm{n}} = 4$ for symmetric nuclear matter) and the second as pions ($m_2 \equiv \overline{m}_\pi = 138$ MeV, $\mu_2 \equiv \mu_\pi = 0$ and $g_2 \equiv g_\pi = 3$). Quantum statistical effects other than the degeneracy factors g_q are neglected. To reproduce experimental data, however, it would be necessary to consider all hadrons and hadronic resonances as well as the contributions from hadronic decays into daughter hadrons.

For some examples the temperature dependence of the relativistic excluded volumes is shown in Fig. 2 (a), given in units of the corresponding non-relativistic terms, $b_{pq} = b_{pq}(0)$. The solid line and the short dashes show the basic excluded volumes $b_{11}(T)$ and $b_{22}(T)$, respectively. In these relative units the decreases of $b_{11}(T)$ and $b_{22}(T)$ depend only on the corresponding masses. It is apparent that the pion excluded volume $b_{22}(T)$ is affected much stronger than the excluded volume of the nucleons, $b_{11}(T)$. The dotted line shows the mixed volume term $b_{12}(T)$, and the long dashes show the compound volume term $D(T) \equiv b_{11}(T) + b_{22}(T) - 2b_{12}(T)$. These two terms depend obviously on both masses and both radii.

The curves for the generalised excluded volume terms of the linear approximation $\tilde{b}_{12}(T)$ and $\tilde{b}_{21}(T)$ behave similarly to $b_{12}(T)$.

Introducing the relativistic excluded volumes $b_{pq}(T)$, however, has two effects. First, the maximum densities become larger since it is generally $1/b_{qq}(T) > 1/b_{qq}$ as seen in Fig. 2 (a). Furthermore, the balance between the lighter and the heavier species is changed because the lighter species is affected more than the heavier at the same temperature: For the above parameters it is $b_{22}(T)/b_{22} \leq b_{11}(T)/b_{11}$.

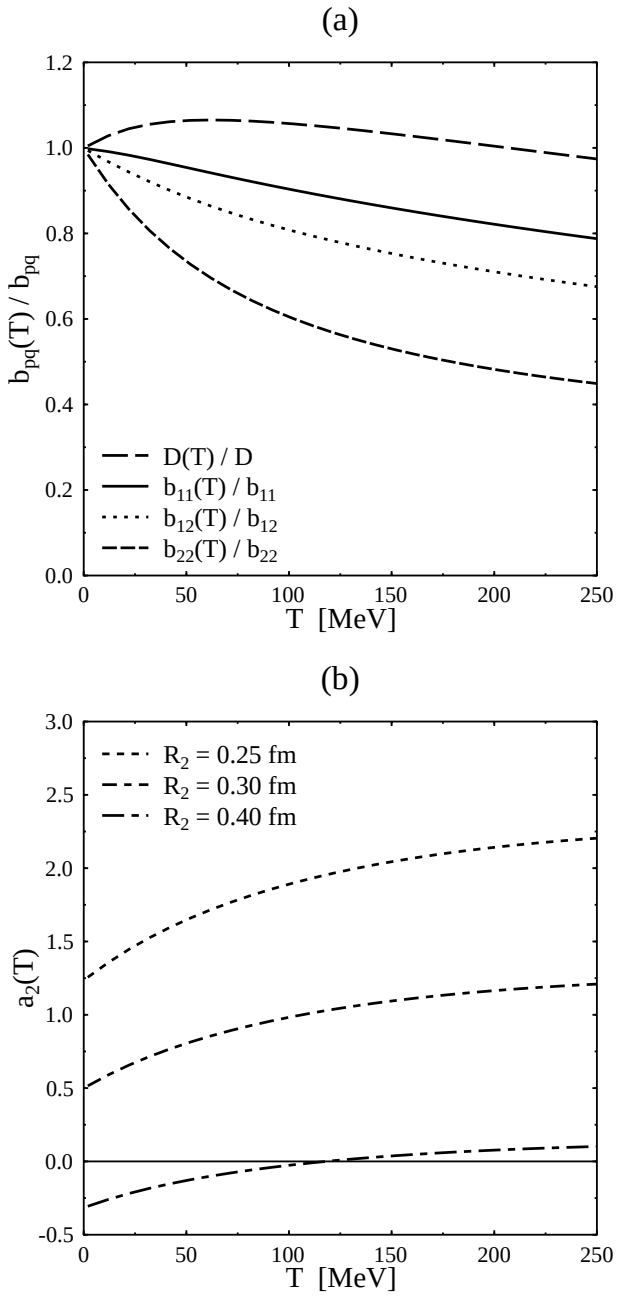

FIG. 2. Temperature dependence of the relativistic excluded volume terms for $m_1 = m_{\rm n}, m_2 = \overline{m}_\pi, R_1 = 0.6$ fm.
(a) Relative values for $R_2 = 0.3$ fm: $b_{11}(T)/b_{11}$, $b_{12}(T)/b_{12}$, $b_{22}(T)/b_{22}$ and $D(T)/D$ (solid line, dotted line, short and long dashes, respectively). The relativistic excluded volume of light species ($b_{22}(T)/b_{22}$) is affected more strongly by temperature.
(b) The characteristic coefficient of the non-linear approximation $a_2(T) = (\sqrt{D(T)/b_{22}(T)} - 1)$ for various $R_2 = 0.25$, 0.3 and 0.4 fm. The non-linear enhancement ($a_2(T) > 0$) becomes stronger due to the decrease of the relativistic excluded volumes with increasing temperature.

In the non-linear approximation this balance is characterised by the coefficient a_2 defined by Eq. (45). In Fig. 2 (b) the temperature dependence of $a_2(T) \equiv (\sqrt{D(T)/b_{22}(T)} - 1)$ is shown for three different values of R_2. The *relativistic* coefficient $a_2(T)$ increases with T, i. e. the non-linear enhancement becomes stronger for higher temperatures. For some values of R_2, e. g. $R_2 = 0.4$ fm, a primary suppression $a_2(0) \equiv a_2 < 0$, turns into an enhancement $a_2(T) > 0$, when the temperature is sufficiently high. For temperature dependent excluded volumes $R_{2,\,\rm crit}$ looses its meaning; here, only $a_2(T) > 0$ is the valid condition for the occurrence of the non-linear enhancement or densities $n_1^{\rm nl} > 1/b_{11}(T)$.

The linear coefficient, $\tilde{a}_2(T) = -2b_{12}(T)/(b_{11}(T) + b_{22}(T))$, is not strongly affected by temperature for the above choice of hadronic parameters: It increases slightly with T but remains negative. Hence, changes in the balance between the lighter and the heavier species play a minor role for the linear approximation.

Particle densities for nucleons and pions in units of $n_0 = 0.16$ fm^{-3} vs. $\mu_1/m_1 \equiv \mu_{\rm n}/m_{\rm n}$ are shown in Figs. 3 (a) and (b) for $T = 185$ MeV. The linear and non-linear results are shown for constant excluded volumes with short dashes and solid lines, respectively, and further for relativistic excluded volumes with dotted lines and long dashes, respectively. At this high temperature the relativistic results are significantly higher than the non-relativistic result. A difference between the linear and the non-linear approximation due to the non-linear enhancement becomes noticeable only for high $\mu_{\rm n}/m_{\rm n} > 0.8$. Thus, for $R_{\rm n} = R_1 = 0.6$ fm from above, the linear and non-linear approximation are practically equivalent for nucleon densities below $n_{\rm n} \approx 0.8\, n_0$, i. e. for densities below about $n_1 \approx 1/(2\, b_{11})$. On the other hand, due to the strong decrease of $b_{22}(T)$ with increasing temperature, the influence of the relativistic excluded volumes is essential for temperatures of the order of $T \approx m_\pi$.

The presence of the additional terms containing temperature derivatives in the energy density (52) or (53) makes it impossible to convert a VdW gas with relativistic excluded volumes into a gas of free streaming particles. Therefore, it is problematic to use these formulae for the post-freeze-out stage. For the latter the quantities of the free streaming particles without any interaction should be used, see discussion in [17,18] and references therein. However, these equations of state may be used to describe the stage between chemical and thermal freeze-out, i. e. a pre-freeze-out stage in terms of Refs. [17,18]. This is examplified in the next section.

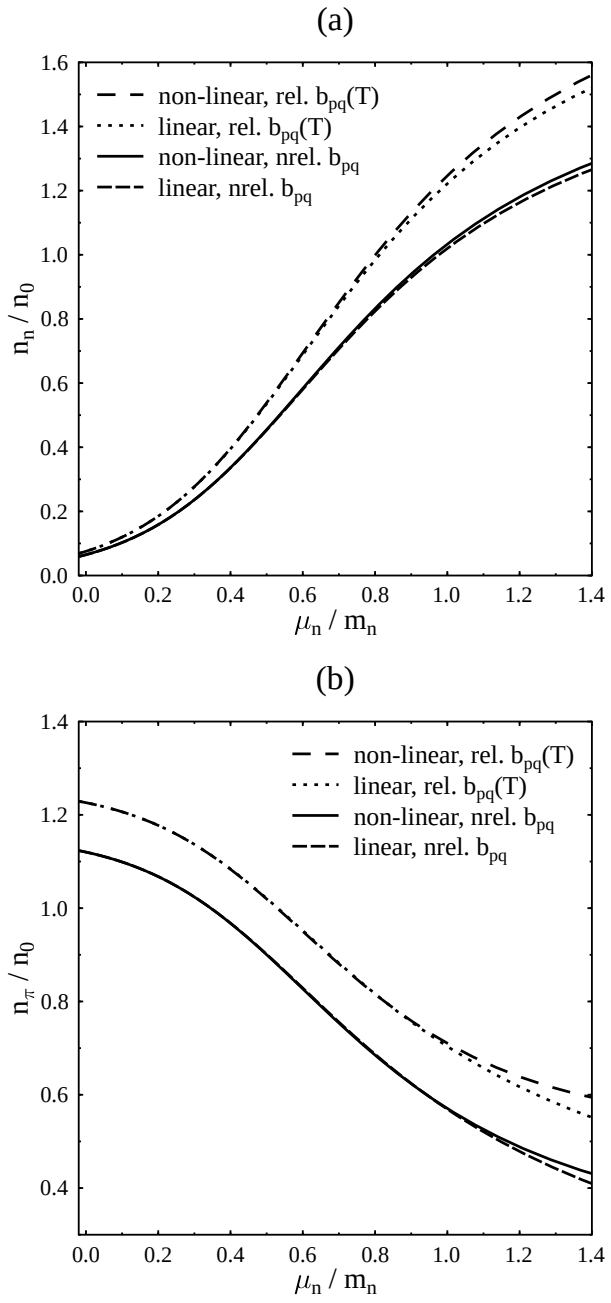

FIG. 3. Comparison of the model predictions for the nucleon (a) and pion (b) density $n_{\rm n}$ and n_π, respectively, vs. $\mu_{\rm n}/m_{\rm n}$ ($R_1 = 0.6$ fm, $R_2 = 0.3$ fm and $T = 185$ MeV, densities in units of $n_0 = 0.16$ fm^{-3}). In both figures the two upper lines correspond to relativistic excluded volumes $b_{pq}(T)$ and the two lower lines to non-relativistic excluded volumes b_{pq}. The results of the linear and non-linear approximation coincide – only for extremely large $\mu_{\rm n}/m_{\rm n}$ the non-linear results lie slightly higher than the corresponding linear results. The deviations due to relativistic excluded volumes are significant.

V. HARD-CORE RADII FROM PARTICLE YIELD RATIOS

As a simple application of the equations of state presented above, let us re-evaluate the thermal model fit parameters for particle yield ratios of Ref. [6], namely the hard-core radii of pions R_π and other hadrons $R_{\rm o}$. A two-component *VdW* excluded volume model has been used there to explain the pion abundance in A+A-collisions by a smaller hard-core radius for the pions than for the other hadrons. The ratios has been fitted to BNL AGS (Au+Au at 11 A GeV) and CERN SPS (Pb+Pb at 160 A GeV) data [7] within a thermal model, including all resonances up to 2 GeV and using quantum statistics.

The applied model, however, corresponds to the incorrect separated model as pointed out in Sect. I. For convenience we give these formulae in *Boltzmann* approximation. Within the previously defined notation the two coupled transcendental equations read

$$\xi_1^{\rm sp}(T,\mu_1,\mu_2) = A_1\, \exp\left[-(\xi_1^{\rm sp}+\xi_2^{\rm sp})\, b_{11}\right] \ , \qquad (55)$$
$$\xi_2^{\rm sp}(T,\mu_1,\mu_2) = A_2\, \exp\left[-(\xi_1^{\rm sp}+\xi_2^{\rm sp})\, b_{22}\right] \ , \qquad (56)$$

wheras $p^{\rm sp}(T,\mu_1,\mu_2) = T\,(\xi_1^{\rm sp}+\xi_2^{\rm sp})$. In this context A_1 represents a sum over the contributions of all hadron species but pions, while A_2 corresponds to the pions only.

The expressions for the particle densities are obtained from $n_q^{\rm sp} \equiv \partial p^{\rm sp}/\partial\mu_q$,

$$n_1^{\rm sp}(T,\mu_1,\mu_2) = \frac{\xi_1^{\rm sp}}{1+\xi_1^{\rm sp} b_{11} + \xi_2^{\rm sp} b_{22}} \ , \qquad (57)$$
$$n_2^{\rm sp}(T,\mu_1,\mu_2) = \frac{\xi_2^{\rm sp}}{1+\xi_1^{\rm sp} b_{11} + \xi_2^{\rm sp} b_{22}} \ . \qquad (58)$$

Solving these equations for $\xi_1^{\rm sp}$ and $\xi_2^{\rm sp}$ one recovers the canonical pressure formula of the separated model (11) as announced in Sect. II.

Due to the separation of both components in this model there is no excluded volume term b_{12} for the interaction between different components at all. This is an essential difference to both the linear and the non-linear approximation. Note that the separated model is *not* a two-component *VdW approximation* because it cannot be obtained by approximating the CPF (13).

The transcendental factors of the formulae (55, 56) exhibit a constant *VdW*-like suppression $\exp[-(p/T)\, b_{qq}]$. There is a reduction of this suppression in the linear and in the non-linear approximation, as discussed in Sect. III. The *VdW*-like suppression is reduced, if b_{12} appears in the corresponding formulae since b_{12} is smaller than b_{11} for $R_2 < R_1$. It is evident that the deviation of the linear and non-linear approximation from the separated model is the larger the more R_1 and R_2 differ from each other.

In the first step of the fit procedure of Ref. [6] only the hadron ratios excluding pions have been taken to find the freeze-out parameters. For AGS $T \approx 140$ MeV, $\mu_{\rm B} \approx 590$ MeV and for SPS $T \approx 185$ MeV, $\mu_{\rm B} \approx 270$

MeV have been obtained. In the second step, a parameter introduced as the *pion effective chemical potential* μ_π^* has been fitted to the pion-to-hadron ratios. Using *Boltzmann* statistics it can be shown that the pion enhancement is thoroughly regulated by the value of μ_π^* [6]; one has obtained $\mu_\pi^* \approx 100$ MeV for AGS and $\mu_\pi^* \approx 180$ MeV for SPS data, respectively.

The pion effective chemical potential depends explicitly on the excluded volumes but also on the pressure. The pressure itself is a transcendental function depending solely on the excluded volumes since T and μ_B are already fixed by step one. In Ref. [6] the formula $\mu_\pi^* \equiv (v_o - v_\pi)\, p(v_o, v_\pi)$ has been obtained for the separated model, where $v_\pi \equiv b_{22}$ and $v_o \equiv b_{11}$ are the excluded volumes corresponding to the hard-core radii of pions $R_\pi \equiv R_2$ and other hadrons $R_o \equiv R_1$, respectively. Thus, the μ_π^* values for AGS and SPS data define two curves in the R_π–R_o-plane. The main conclusion of Ref. [6] is that the intersection point of these two curves ($R_\pi = 0.62$ fm, $R_o = 0.8$ fm) gives the correct pair of hard-core radii for pions and for the other hadrons, i. e. AGS and SPS data are fitted simultaneously within the applied model.

In Ref. [8] these values of R_o and R_π have been criticised for being unreasonably large. There, a complete fit of solely SPS data has been performed within a separated model. The best fit has been obtained for equal hard-core radii, $R_\pi = R_o = 0.3$ fm, motivated by nucleon scattering data. Good agreement has been found as well for a *baryon* hard-core radius, $R_{Bar} = 0.3$ fm, and a common hard-core radius for *all mesons*, $R_{Mes} = 0.25$ fm, choosen in accord with the above ratio of radii, $R_o/R_\pi = 0.8/0.62$. Larger hard-core radii, especially those of Ref. [6], are quoted as giving distinctly worse agreement.

Assuming the validity of *Boltzmann* statistics, we have re-calculated the $R_o(R_\pi)$-curves for the above μ_π^* values; firstly in the separated model (55–58), i. e. as presented in [6]. The resulting curves, shown as thin lines in Fig. 4 (a), naturally match the results of the underlying fit of Ref. [6], which are indicated by markers.

Then we have considered the linear and the non-linear approximation. Due to the occurence of b_{12} terms in these two cases, both functional forms of μ_π^* are essentially different from the separated case. Consequently, the shapes of the $R_o(R_\pi)$-curves are different as well. We find distinct deviations from the separated model, especially for $R_\pi \to 0$, and the values for the intersection point are slightly lower; see thin lines in Fig. 4 (b) for the linear exrapolation. The non-linear approximation gives identical results for this purpose because the hadron densities are too small for a noticeable non-linear enhancement.

The crucial point is now to turn on the relativistic temperature dependence of the excluded volumes. To keep the analysis simple we treat only pions this way since they give the strongest effect.

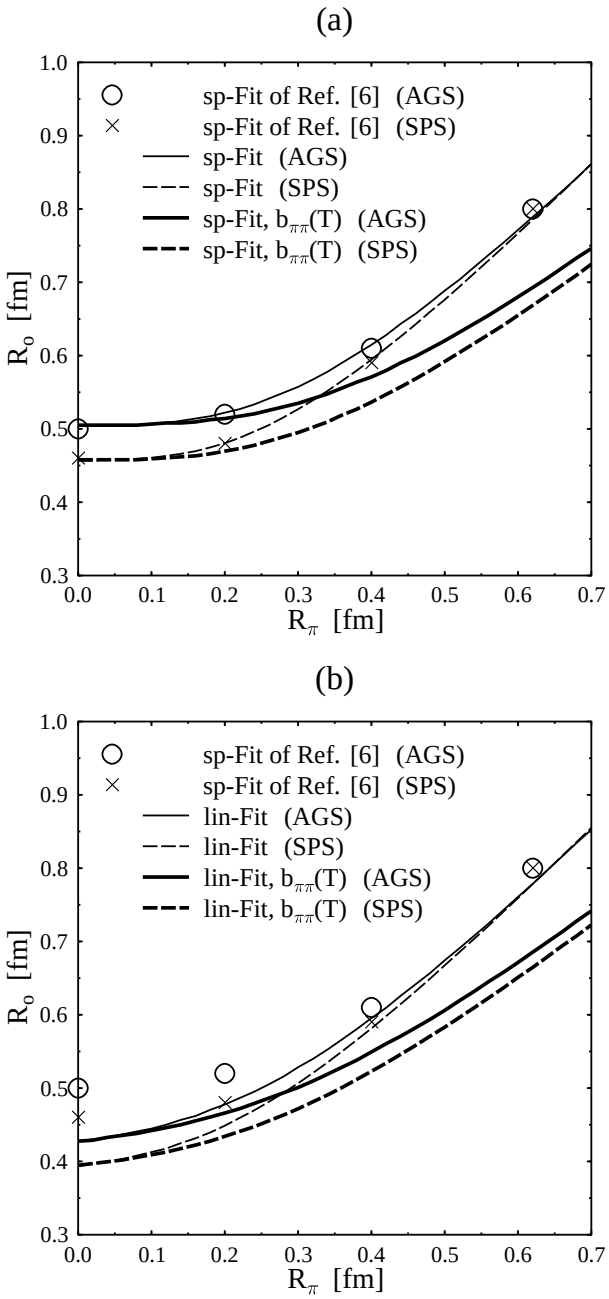

FIG. 4. Fits of particle yield ratios for AGS and SPS data [7] with the separated model and the linear approximation. The thin lines show the fits for the separated model (a) and the linear approximation (b); the non-linear approximation gives identical results for the latter case.
The thick lines in (a) and (b) show the corresponding curves for relativistic excluded volumes $v_\pi = b_{22}(T)$: there is no intersection for either of the three models. In both figures the results of the fit from Ref. [6] for AGS and SPS data are indicated by circles and crosses, respectively.

Although the other hadrons are assumed to have equal hard-core radii, their relativistic excluded volumes would be different for $T > 0$, according to their different masses. To check the influence of relativistic excluded volumes for *all* particles, we have used *one average* mass of 1 GeV for *all other* hadrons. The corresponding change in the $R_{\rm o}$-values are below 5%.

The results of the fit for relativistic excluded volumes for pions are shown in Figs. 4 (a) and (b) as thick lines. Though this approach is more realistic, there is *no* intersection point for *any* of the three models even for very large radii $R_{\rm o}, R_\pi \gg 0.5$ fm. For the approximated case of a single averaged hadron mass there is no intersection either. Because of the different freeze-out temperatures for AGS and SPS the $v_\pi(T) \equiv b_{22}(T)$ values are changed differently in both cases, and so are the scales for the corresponding R_π.

Due to the errors in experimental data one ought to obtain a corridor instead of a curve for each set of data. Consequently, the particle yield ratios can be reproduced well by e. g. $R_{\rm o} \approx 0.4$ fm, $R_\pi \approx 0.2$ fm or larger values for any of the models with relativistic excluded volumes. Therefore, we conclude that the fit procedure proposed in Ref. [6] is *not* suitable to find a *unique* pair of hard-core radii for pions and other hadrons, as long as a best fit is searched for just two sets of data of particle yield ratios. The use of a relativistic excluded volume for pions along with a correct approximation reduce the value of the necessary nucleon hard-core radius essentially towards more realistic values.

VI. SUMMARY

In the present work several equations of state for the two-component *Van der Waals* excluded volume model are derived and investigated. We have discussed two essentially different formulations, the linear and the non-linear approximation.

The non-linear approximation is the simplest possibility. Here, the large component can reach higher densities n_1 than the usual limiting *VdW* density $1/b_{11}$, if the other component has a suffiently small hard-core radius, $R_2 < R_{2,\,\rm crit}$. In the linear approximation the densities cannot exceed the usual limiting *VdW* densities $1/b_{11}$ and $1/b_{22}$, but generalised excluded volume terms have to be introduced.

For both approximations the suppression factors of the grand canonical formulae contain a *VdW*-like term, proportional to $\exp[-(p/T)\, b_{qq}]$, which however is reduced non-trivially. In the linear case there is a slight reduction, wheras in the non-linear case this reduction can turn the suppression even into an enhancement for the smaller component, which leads to exceeding of $1/b_{11}$ for the density of the larger component n_1.

The commonly used formulae of the separated model are shown to be not suitable for the two-component case, because they correspond to a system where both components are separated from each other and cannot mix. In this model the grand canonical suppression factor is just *VdW*-like and has no reduction of the suppression.

Furthermore relativistic, i. e. *Lorentz*-contracted, excluded volumes have been introduced. Naturally, the relativistic excluded volume per particle decreases with rising temperature. This effect is the stronger the lighter the particle species is. The suppression of particle densities in *VdW* models is lower for a component of smaller excluded volume in comparison with a component of larger excluded volume. Therefore, the temperature dependence of the relativistic excluded volumes causes a reduction of the particle densities suppression.

The full equations of state have been presented, for both the linear and non-linear approximation, with constant and with relativistic excluded volumes. For the entropy density and energy density there are additional terms containing temperature derivatives of the relativistic excluded volume terms due to their 'thermal compressibility'. In comparison with the non-relativistic case, the expressions for the pressure and the particle densities remain unchanged, but the possible range of values is obviously wider, since it is generally $1/b_{11}(T) \geq 1/b_{11}$ and $1/b_{22}(T) \geq 1/b_{22}$.

As an application of the derived formulations a fit of particle yield ratios for SPS and AGS has been re-evaluated. In Ref. [6] this fit had been done in a separated model by adjusting the hard-core radii for the pions R_π and for the other hadrons $R_{\rm o}$. The results of the new fit are essentially different from the separated model but coincide for both the linear and non-linear approximation. The picture changes drastically, however, if relativistic excluded volumes are adopted for pions. The basic idea of the fit – one pair of hard-core radii suffices to fit AGS and SPS data simultaneously – does not lead to a result anymore. This is the case for the separated model and for both approximations, linear and non-linear. Experimental uncertainties lead to a *region* of possible values in the $R_{\rm o}$–R_π-plane; one could describe the data for $R_{\rm o} \geq 0.4$ fm and $R_\pi \geq 0.2$ fm.

We conclude that there are two causes of an *enhancement* of particle densities, e. g. the thermal pion abundance, in *VdW* descriptions: First, the density suppression is generally lower for the smaller component in two-component models. Second, there is a further reduction of the density suppression due to the relativistic excluded volumes. The latter are essentially smaller for light hadron species than for heavy species, especially for temperatures $T \gg 50$ MeV.

When applied to the hadron gas, the linear and non-linear results almost coincide for nucleon densities up to $n_0 \approx 0.16$ fm^{-3} (for $R_{\rm o} \leq 0.6$ fm) since the non-linear enhancement does not appear there, but the deviation from the incorrect separated model is distinct. However, the formulae of the non-linear approximation are essentially simpler than these of the linear approximation.

The influence of relativistic effects on the excluded vol-

umes becomes indispensable for temperatures typical for heavy ion collisions. Therefore, it is necessary to include a correct two- or multi-component VdW approximation – linear or non-linear – as well as relativistic excluded volumes in future calculations.

ACKNOWLEDGMENTS

The authors thank M. I. Gorenstein and D. H. Rischke for useful discussions and St. Hofmann for valuable comments.

The financial support of the NATO Linkage Grant PST.CLG.976950 is acknowledged.

APPENDIX A: THE TWO VDW APPROXIMATIONS IN THE CE

In the following we will study the differences between the linear and the non-linear approximation: the total excluded volumes $v_q = v_q(N_1, N_2)$ of the corresponding partial pressures. In the linear pressure formula (20) each component has its own total excluded volume given by

$$v_1^{\rm lin} \equiv N_1 b_{11} + N_2 \tilde{b}_{21} \ , \quad v_2^{\rm lin} \equiv N_1 \tilde{b}_{12} + N_2 b_{22} \ , \quad \text{(A1)}$$

whereas in the non-linear pressure formula (17) there is a *common* total excluded volume for both components

$$v_1^{\rm nl} = v_2^{\rm nl} = v^{\,\rm nl} \equiv N_1 b_{11} + N_2 b_{22} - \tfrac{N_1 N_2}{N_1 + N_2} D \ . \quad \text{(A2)}$$

It can be readily checked that it is either $v_1^{\rm lin} \le v^{\,\rm nl} \le v_2^{\rm lin}$ or $v_1^{\rm lin} \ge v^{\,\rm nl} \ge v_2^{\rm lin}$, i. e. the pole of the non-linear pressure always lies between both poles of the linear pressure. Hence, there are values N_1, N_2, where the non-linear pressure is still finite, but the linear pressure formula is yet invalid since one of the partial pressures has already become infinite. Consequently, the domain of the non-linear approximation is larger.

For given V the two domains can be expressed by the limiting densities (22) and (23), which are defined by the poles $v_q(N_1, N_2) = V$ of the corresponding pressure. In the linear approximation one obtains the expressions

$$\hat{n}_{1,1}^{\rm lin}(n_2) = \frac{1 - \tilde{b}_{21} n_2}{b_{11}} \ , \quad \hat{n}_{1,2}^{\rm lin}(n_2) = \frac{1 - b_{22} n_2}{\tilde{b}_{12}} \ . \quad \text{(A3)}$$

For given n_2, therefore, the domain of $p^{\,\rm lin}$ (20) is

$$0 \le n_1^{\rm lin} < \min\left\{ \hat{n}_{1,1}^{\rm lin}(n_2) \, , \ \hat{n}_{1,2}^{\rm lin}(n_2) \right\} \ . \quad \text{(A4)}$$

In the non-linear approximation there is solely one limiting density

$$\hat{n}_1^{\rm nl}(n_2) = \tfrac{1 - 2\, b_{12} n_2 + \sqrt{(1 - 2 b_{12} n_2)^2 + 4 b_{11} n_2 \, (1 - b_{22} n_2)}}{2\, b_{11}} \ . \quad \text{(A5)}$$

Consequently, for given n_2 the domain of $p^{\,\rm nl}$ (17) is

$$0 \le n_1^{\rm nl} < \hat{n}_1^{\rm nl}(n_2) \ . \quad \text{(A6)}$$

In the non-linear approximation there is furthermore a region where the pressure has negative partial derivatives with respect to the smaller particles' number, $\partial p^{\,\rm nl} / \partial N_2 < 0$. The condition $\partial p^{\,\rm nl} / \partial N_2 = 0$ defines the boundary of this region

$$\hat{n}_1^{\rm nl,\,bd}(n_2) = \tfrac{1 - 2\,(b_{12} - b_{22})\, n_2 + \sqrt{(1 - 2\,(b_{12} - b_{22})\, n_2)^2 + 8\,(b_{11} - b_{12})\, n_2}}{4\,(b_{11} - b_{12})} \ . \quad \text{(A7)}$$

For given n_2 a negative derivative $\partial p^{\,\rm nl} / \partial N_2 < 0$ occurs only at a density $n_1 > \hat{n}_1^{\rm nl,\,bd}$, while the derivative $\partial p^{\,\rm nl} / \partial N_1$ is always positive for $R_2 \le R_1$ as readily checked.

In Fig. 1 (a) the functions $\hat{n}_1(n_2)$ are presented in *dimensionless* variables $\hat{n}_1 b_{11}$ and $n_2 b_{22}$. The properties of these dimensionless functions depend only on the ratio of the two radii R_2/R_1. The smaller this ratio is, the higher is the maximum value of $\hat{n}_1^{\rm nl}$, while the region of negative derivatives $\partial p^{\,\rm nl} / \partial N_2$ becomes narrower. The straight line $\hat{n}_{1,1}^{\rm lin}(n_2)$ starts always at $1/b_{11}$, but its slope decreases for smaller R_2/R_1, whereas $\hat{n}_{1,2}^{\rm lin}(n_2)$ ends at $1/b_{22}$ and its slope increases. The pressure of the *separated model* (11) would yield one straight line from $n_1 b_{11} = 1$ to $n_2 b_{22} = 1$ in Fig. 1 (a), for any ratio of the radii R_1 and R_2.

For very small ratios R_2/R_1, i. e. for $R_2 \to 0$, one finds from Eq. (A2) that $v^{\,\rm nl} \to N_1 b_{11} \, [1 - \frac{3}{4} N_2/(N_1 + N_2)]$. This yields the maximum density $\max(\hat{n}_1^{\rm nl}) = 4/b_{11}$ for $N_2 \gg N_1$. Thus $\hat{n}_1^{\rm nl}$ exceeds the maximum density of the linear approximation or of the corresponding one-component VdW gas, $\max(\hat{n}_{1,1}^{\rm lin}) = \max(n_1^{\rm oc}) = 1/b_{11}$, by a factor of four in this case.

Note that the value $4/b_{11}$ appears in the linear approximation as well: For $v_2^{\rm lin} \to V$ it is $\max(\hat{n}_{1,2}^{\rm lin}) = 4/b_{11}$ at $n_2 = 0$, but this density cannot be achieved because $p_1^{\rm lin}(n_1, n_2)$ is infinite for $n_1 \ge 1/b_{11}$.

Let us consider now the consequences of negative derivatives $\partial p^{\,\rm nl} / \partial N_2 < 0$ in the non-linear approximation. If a negative $\partial p^{\,\rm nl} / \partial N_2$ occurs for a density $n_1' = $ const. at $n_2 = 0$, the pressure $p^{\,\rm nl}(n_1', n_2)$ has a minimum at a certain density $n_{2,\,\rm min} > 0$, which is determined by the boundary $\hat{n}_1^{\rm nl,\,bd}(n_2)$. For increasing n_1 along the boundary, consequently, the non-linear pressure is always lower than for increasing n_1 at fixed $n_2 = 0$. Hence along the boundary higher densities can be achieved, in particular $n_1 > 1/b_{11}$.

Therefore, exceeding of $n_1^{\rm nl} = 1/b_{11}$ requires that the boundary starts inside the the non-linear domain at $n_2 = 0$. Thus the condition $\hat{n}_1^{\rm nl,\,bd}(0) < 1/b_{11}$ provides the critical radius $R_{2,\,\rm crit}$ (24),

$$b_{11} < 2 b_{12} \quad \rightsquigarrow \quad R_{2,\,\rm crit}(R_1) = (\sqrt[3]{4} - 1)\, R_1 \ . \quad \text{(A8)}$$

On the other hand the boundary starts at $n_1 = 8/(14\, b_{11})$ for $R_2 \to 0$ at $n_2 = 0$, i. e. for any density $b_{11} n_1 \le$

$8/14 \approx 1/2$ negative values of $\partial p^{\,\mathrm{nl}}/\partial N_2$ do not occur for any radii.

Although it is pathological that for *high* densities n_1 the non-linear pressure firstly decreases, if particles of the second and smaller component are added to the system, there is a reasonable explanation for the lowered pressure along the boundary (A7) for small radii $R_2 < R_{2,\,\mathrm{crit}}$.

Consider, for instance, $n_1 b_{11} = 0.9$ in Fig. 1 (a). Since it is $R_2/R_1 = 0.4$, the dimensionless density of the small particles at the boundary $\hat{n}_1^{\,\mathrm{nl,\,bd}}(n_2)$ nearly vanishes, $n_2 b_{22} \approx 0.05$, whereas the absolute amounts of the small and large particles are about equal. For the excluded volume interaction of the large particles in the pressure formula (17), therefore, the influence of the mixed term b_{12} becomes comparable to that of the distinctly larger non-mixed term b_{11}.

For $R_2/R_1 \ll 1$ one obtains $n_2 \gg n_1$ near the boundary at $n_1 b_{11} = 0.9$, i. e. the large particles are completely surrounded by the smaller particles and interact mostly with these but hardly with other large particles anymore. In this situation, consequently, the excluded volume interaction of the large particles is governed by the essentially smaller b_{12} and not by $b_{11} \leq 8\, b_{12}$.

One might interprete this behaviour as an effective attraction between small and large particles, but it is rather a strong reduction of the large particles' excluded volume suppression.

As VdW approximations are low density approximations they coincide for these densities, but they evidently become inadequate near the limiting densities: both discussed formulations do evidently not match the real *gas of rigid spheres* there.

For high densities the linear approximation behaves natural, i. e. it is $\partial p^{\,\mathrm{lin}}/\partial N_q > 0$ always. However, one has to introduce the additional terms $\tilde{b}_{12}$ and $\tilde{b}_{21}$. For the choice (21) these terms provide a one-component-like behaviour in the limits $R_2 = R_1$ and $R_2 = 0$, but they have no concrete physical meaning.

In the non-linear approximation there occur pathologic pressure derivatives $\partial p^{\,\mathrm{nl}}/\partial N_2 < 0$ for $R_2 \ll R_1$. However, the non-linear formulae may be used for special purposes, e. g. for $n_1 > 1/b_{11}$ at intermediate $n_2 b_{22}$, where the linear approximation is yet invalid.

APPENDIX B: STABILITY OF THE NON-LINEAR APPROXIMATION

The non-linear enhancement in the GCE or the occurence of negative values for $\partial p^{\,\mathrm{nl}}/\partial N_q$ in the CE suggest a further investigation concerning the thermodynamical stability of the non-linear approximation.

One can readily check that in the CE it is $\partial p^{\,\mathrm{nl}}/\partial V < 0$ generally, so there is no *mechanical* instability. To investigate wether there is a *chemical* instability [19] it is necessary to study partial derivatives with respect to the particle numbers, $\partial/\partial N_q$, of the *chemical potentials*

$$\mu_p(T,V,N_1,N_2) \equiv -T\,\tfrac{\partial}{\partial N_p}\,\ln[Z(T,V,N_1,N_2)]\;. \qquad \text{(B1)}$$

Partial derivatives of the *pressure* with respect to the particle numbers $\partial p/\partial N_q$ have no relevance here.

For the examination of chemical stability it is appropriate to switch from the *free energy* of the CE, $F(T,V,N_1,N_2) \equiv -T\,\ln[Z(T,V,N_1,N_2)]$, to the *Gibbs free energy* or *free enthalpie*

$$G(T,p,N_1,N_2) \equiv F + p\,V = \mu_1 N_1 + \mu_2 N_2\;, \qquad \text{(B2)}$$

where $\mu_q(T,p,N_1,N_2) \equiv \partial G/\partial N_q$. This requires that $p(T,V,N_1,N_2)$ can be solved for $V(T,p,N_1,N_2)$, which is the case for the non-linear approximation,

$$V^{\,\mathrm{nl}}(T,p,N_1,N_2) = \tfrac{N_1+N_2}{p/T} + N_1 b_{11} + N_2 b_{22} - \tfrac{N_1\,N_2}{N_1+N_2} D\,.$$

Further it is useful to introduce the molar free enthalpie $g \equiv G/(N_1+N_2) = g(T,p,x_1)$ with the molar fractions $x_1 \equiv N_1/(N_1+N_2)$ and $(1-x_1) = x_2 \equiv N_2/(N_1+N_2)$ of component 1 and 2, respectively. Then the chemical stability of a binary mixture [19] corresponds to the condition

$$\tfrac{\partial^2}{\partial x_1^2}\, g(T,p,x_1) = \tfrac{\partial \mu_1(T,p,x_1)}{\partial x_1} - \tfrac{\partial \mu_2(T,p,x_1)}{\partial x_1} > 0\;. \qquad \text{(B3)}$$

For the non-linear approximation one obtains

$$\begin{aligned} g^{\,\mathrm{nl}}&(T,p,x_1) \\ &= x_1 \left\{ T\,\ln\left[\tfrac{x_1}{\phi_1}\tfrac{p}{T}\right] + p\left(b_{11} - (1-x_1)^2\, D\right)\right\} \qquad \text{(B4)} \\ &\quad + (1-x_1)\left\{ T\,\ln\left[\tfrac{1-x_1}{\phi_2}\tfrac{p}{T}\right] + p\left(b_{22} - x_1^2\, D\right)\right\}\;, \end{aligned}$$

and thus condition (B3) is satisfied:

$$\tfrac{\partial^2}{\partial x_1^2}\, g^{\,\mathrm{nl}}(T,p,x_1) = \tfrac{T}{x_1} + \tfrac{T}{1-x_1} + p\,2D > 0\;. \qquad \text{(B5)}$$

Therefore, the system described by the non-linear approximation is thermodynamically stable – despite the pathologic behaviour in special cases. Due to the equivalence of the thermodynamical ensembles this is true for any representation of the model.

APPENDIX C: THE TWO VDW APPROXIMATIONS IN THE GCE

In this part we will study the non-linear and the linear approximation in the grand canonical ensemble. As in the CE the differences between the linear and non-linear approximation occur only for high densities of the larger particles, n_q, which correspond to large chemical potentials μ_q in the grand canonical treatment. Therefore, we will study the limit given by Eq. (44): $\mu_1/T \to \infty$ for constant T, μ_2 and $R_2 \leq R_1$, where it is $\xi_1 \to \infty$.

The *transcendental exponents* of both approximations contain an *attractive* part besides the usual VdW-like

suppressive part $\exp[-(p/T)\,b_{qq}]$: In the linear approximation (36, 37) the suppression is reduced, but the transcendental exponents are always negative – whereas the suppression in the non-linear approximation (29, 30) is not only reduced, but the transcendental exponent of $\xi_2^{\rm nl}$ can even become positive in the above limit.

To examine the latter we rewrite the coupled transcendental equations (29, 30) as

$$\xi_1^{\rm nl} = \phi_1 \, \exp\left[\tfrac{\mu_1}{T}\right] \times \qquad \text{(C1)}$$
$$\times \exp\left[-\left(\xi_1^{\rm nl}+\xi_2^{\rm nl}\right) b_{11} \, \left(1 - \tfrac{D/b_{11}}{(\xi_1^{\rm nl}/\xi_2^{\rm nl}+1)^2}\right)\right] ,$$
$$\xi_2^{\rm nl} = \phi_2 \, \exp\left[\tfrac{\mu_2}{T}\right] \times \qquad \text{(C2)}$$
$$\times \exp\left[-\left(\xi_1^{\rm nl}+\xi_2^{\rm nl}\right) b_{22} \, \left(1 - \tfrac{D/b_{22}}{(1+\xi_2^{\rm nl}/\xi_1^{\rm nl})^2}\right)\right] .$$

If R_2 is sufficiently smaller than R_1, then D/b_{22} is larger than unity and the transcendental exponent of $\xi_2^{\rm nl}$ (C2) can become positive,

$$0 < \tfrac{D}{b_{22}} - \left(1+\tfrac{\xi_2^{\rm nl}}{\xi_1^{\rm nl}}\right)^2$$
$$\iff \tfrac{\xi_2^{\rm nl}}{\xi_1^{\rm nl}} < a_2 \equiv \sqrt{\tfrac{D}{b_{22}}} - 1 \, . \qquad \text{(C3)}$$

The coefficient $a_2 = a_2(R_1/R_2)$ introduced here is the crucial combination of excluded volumes in the non-linear approximation. It characterises the behaviour of this approximation in the limit (44), i. e. for $\xi_1 \to \infty$.

For equal radii $R_2 = R_1$ it is $a_2 = -1$, and one has full *VdW*-like suppression, $\propto \exp[-(p/T)\,b_{qq}]$. Negative a_2 indicate the strength of suppression of $\xi_2^{\rm nl}$ for increasing $\xi_1^{\rm nl}$. For $-1 < a_2 < 0$ the suppression is reduced, most strongly for $a_2 \approx 0$. In the case $a_2 = 0$ there is no suppression in the limit (44) but $\xi_2^{\rm nl} \to A_2 = $ const. for $\xi_1^{\rm nl} \to \infty$. Thus, the condition $a_2 = 0$ provides the critical radius,

$$D/b_{22} = 1 \quad \iff \quad R_{2,\,\rm crit} = (\sqrt[3]{4} - 1)\, R_1 \, , \qquad \text{(C4)}$$

which coincides with the canonical result (A8).

For positive a_2 or $R_2 < R_{2,\,\rm crit}$ the *non-linear enhancement* occurs: $\xi_2^{\rm nl}$ is enhanced by increasing $\xi_1^{\rm nl}$ as long as the second exponent in (C2) is positive, i. e. for $\xi_2^{\rm nl} < a_2\, \xi_1^{\rm nl}$. The transcendental factor of $\xi_1^{\rm nl}$ (C1) has only a reduced suppression in this case. According to Eq. (C3) one obtains

$$\xi_2^{\rm nl} \to a_2\, \xi_1^{\rm nl} \, , \qquad \text{but also} \qquad n_2^{\rm nl} \to a_2\, n_1^{\rm nl} \, , \qquad \text{(C5)}$$

since it is $n_2^{\rm nl}/n_1^{\rm nl} = \xi_2^{\rm nl}/\xi_1^{\rm nl}$ due to Eqs. (33, 34).

Using Eqs. (C5) and (C3) one obtains for the particle densities (33, 34)

$$n_1^{\rm nl} \to \tfrac{1}{b_{11} - a_2^2\, b_{22}} = \tfrac{1}{b_{11} - (\sqrt{D} - \sqrt{b_{22}})^2} \, , \qquad \text{(C6)}$$
$$n_2^{\rm nl} \to a_2\, n_1^{\rm nl}$$
$$\to \tfrac{a_2}{b_{11} - a_2^2\, b_{22}} = \tfrac{\sqrt{b_{22}}}{b_{22}} \, \tfrac{\sqrt{D} - \sqrt{b_{22}}}{b_{11} - (\sqrt{D} - \sqrt{b_{22}})^2} \, . \qquad \text{(C7)}$$

It is clearly seen that the density $n_1^{\rm nl}$ can exceed $1/b_{11}$ for positive a_2. As in the CE the maximum value, $\max(n_1^{\rm nl}) = 4/b_{11}$, is achieved for $R_2 = 0$ or $a_2 = \infty$. Then, in the limit (44) the density of the second component diverges, $n_2^{\rm nl} \to \infty$, but its total excluded volume vanishes, $n_2^{\rm nl}\, b_{22} \to 0$, as seen from Eq. (C7).

There is yet another case, where the condition (C3) is fulfilled, the *early enhancement*: $\xi_2^{\rm nl}$ can be enhanced with increasing μ_2 for constant T and μ_1, if μ_1 is sufficiently large. This enhancement takes place only at small μ_2, and it obviously vanishes when μ_2 is large enough so that $\xi_2^{\rm nl} \geq a_2 \xi_1^{\rm nl}$. The early enhancement is the direct analogue to a negative derivative $\partial p^{\rm nl}/\partial N_q < 0$ in the CE.

The coupled transcendental equations of the linear approximation (36, 37) may be rewritten similarly to Eqs. (C1, C2). For the choice (21) one obtains in terms of D from Eq. (16)

$$\xi_1^{\rm lin}(T,\mu_1,\mu_2) \qquad \text{(C8)}$$
$$= A_1 \, \exp\left[-\left(\xi_1^{\rm lin}+\xi_2^{\rm lin}\right) b_{11} \left(1 - \tfrac{\xi_2^{\rm lin}}{\xi_1^{\rm lin}+\xi_2^{\rm lin}} \tfrac{D}{b_{11}+b_{22}}\right)\right] ,$$
$$\xi_2^{\rm lin}(T,\mu_1,\mu_2) \qquad \text{(C9)}$$
$$= A_2 \, \exp\left[-\left(\xi_1^{\rm lin}+\xi_2^{\rm lin}\right) b_{22} \left(1 - \tfrac{\xi_1^{\rm lin}}{\xi_1^{\rm lin}+\xi_2^{\rm lin}} \tfrac{D}{b_{11}+b_{22}}\right)\right] .$$

In this case the condition for the enhancement of $\xi_2^{\rm lin}$ for $R_2 \leq R_1$ would be

$$\tfrac{\xi_2^{\rm lin}}{\xi_1^{\rm lin}} < \tilde{a}_2 \equiv -\tfrac{2b_{12}}{b_{11}+b_{22}} \, . \qquad \text{(C10)}$$

As $\tilde{a}_2$ is always negative the *VdW*-like suppression is only reduced in this approximation. Like in the non-linear approximation $\tilde{a}_2 = -1$ corresponds to equal radii $R_2 = R_1$ and full *VdW*-like suppresion, whereas $\tilde{a}_2 = -1/4$ ($R_2 = 0$) corresponds to the most strongly reduced suppresion in the linear approximation.

Thus, the densities $n_q^{\rm lin}$ can not exceed the maximum value $1/b_{qq}$ of the corresponding one-component case. Furthermore, the density $n_2^{\rm lin}$ (41) vanishes in the analogous limit to (44), $\xi_1^{\rm lin} \to \infty$, in contrast to the non-linear behaviour.

In the case $R_1 \leq R_2$ one would evidently investigate the coefficients $a_1 \equiv (\sqrt{D/b_{11}} - 1)$ in the non-linear and $\tilde{a}_1 \equiv -(2b_{12})/(b_{11}+b_{22}) = \tilde{a}_2$ in the linear approximation, respectively.

[1] H. Stöcker, W. Greiner and W. Scheid *Z. Phys.* A **286** (1978) 121;
H. Stöcker and W. Greiner *Phys. Rep.* **137** (1986) 277;
C. Greiner and H. Stöcker *Phys. Rev.* D **44** (1991) 3517.

[2] P. Koch, B. Müller and J. Rafelski *Phys. Rep.* **142** (1986) 167;

J. Letessier, A. Tounsi, U. W. Heinz, J. Sollfrank and J. Rafelski *Phys. Rev. Lett.* **70** (1993) 3530 .
[3] J. Cleymans and H. Satz *Z. Phys.* C **57** (1993) 135 ; J. Cleymans and K. Redlich *Phys. Rev. Lett.* **81** (1998) 5284 .
[4] P. Braun-Munzinger, J. Stachel, J. P. Wessels and N. Xu *Phys. Lett.* B **344** (1995) 43 *and* B **365** (1996) 1 .
[5] F. Becattini and U. W. Heinz, *Z. Phys.* C **76** (1997) 269 .
[6] G. D. Yen, M. I. Gorenstein, W. Greiner and S. N. Yang *Phys. Rev.* C **56** (1997) 2210 .
[7] Proceedings of the Quark Matter '96 *Nucl. Phys.* A **610** (1996) 1c .
[8] P. Braun-Munzinger, I. Heppe and J. Stachel *Phys. Lett.* B **465** (1999) 15 .
[9] J. D. van der Waals *Z. Phys. Chem.* **5** (1889) 133 .
[10] H. A. Lorentz *Ann. Physik* **12** (1881) 127 .
[11] D. Berthelot *Compt. Rend.* **126** (1898) 1703 *and* 1857 .
[12] A. Münster: "Statistical Thermodynamics" Vol. II , Springer-Verlag, Heidelberg 1974, 581 .
[13] M. I. Gorenstein, A. P. Kostyuk and Y. D. Krivenko *J. Phys.* G **25** (1999) L75 .
[14] K. A. Bugaev, M. I. Gorenstein, H. Stöcker and W. Greiner *Phys. Lett.* B **485** (2000) 121 .
[15] K. A. Bugaev and D. H. Rischke *(in preparation)* 15 p.
[16] G. Zeeb: Diploma thesis, Frankfurt am Main 2002 .
[17] K. A. Bugaev *Nucl. Phys.* A **606** (1996) 559 ; K. A. Bugaev and M. I. Gorenstein *(Preprint)* arXiv:nucl-th/9903072 ; K. A. Bugaev, M. I. Gorenstein and W. Greiner *J. Phys.* G **25** (1999) 2147 *and Heavy Ion Phys.* **10** (1999) 333 .
[18] V. K. Magas *et al. Nucl. Phys.* A **661** (1999) 596 ; C. Anderlik *et al. Phys. Rev.* C **59** (1999) 3309 ; V. K. Magas *et al.*, *Heavy Ion Phys.* **9** (1999) 193 .
[19] L. E. Reichl: "A Modern Course in Statistical Physics", 2nd Edition, J. Wiley & Sons, New York 1998, 55 , 153 .